Journal of Atmospheric and Solar-Terrestrial Physics 70 (2008) 1929–1934

Contents lists available at ScienceDirect

Journal of Atmospheric and Solar-Terrestrial Physics

journal homepage: www.elsevier.com/locate/jastp

Removing multiple reflections from the F2 layer to improve Autoscala performance

Carlo Scotto *, Michael Pezzopane

Istituto Nazionale di Geofisica e Vulcanologia, Via di Vigna Murata 605, 00143, Rome, Italy

ARTICLE INFO

Article history:
Accepted 17 May 2008
Available online 1 June 2008

Keywords:
Ionospheric monitoring
Ionosonde
Autoscala
Ionogram autoscaling

ABSTRACT

This work describes a simple filter able to eliminate the traces caused by second-order reflection from ionograms. This filter is applied to Autoscala in order to smooth out cases in which the autoscaling of the ionogram is mistaken because the second-order F2 layer reflection is identified as first order. A dataset of 32,626 ionograms recorded at the ionospheric observatory of Rome was used to test the filter.

1. Introduction

One of the longest standing techniques for carrying out ionospheric ground-based observations is vertical sounding with an ionosonde. The principle of this technique is to transmit radio pulses, with carrier frequency typically varied from 1 to 20 MHz, vertically towards the ionosphere and record the time that elapses before the echo is received. Traditionally, in place of time delay the virtual height is plotted against the frequency and this record is referred to as an ionogram. When analysing an ionogram several important parameters can be identified of significance for space weather purposes, making ionogram analysis one of the most significant ways to monitor and study ionospheric storms. These are the sum of solar–terrestrial events starting in many cases with a coronal mass ejection followed by its transit from the Sun to the Earth and the subsequent coupling of its energy and mass to the magnetospheric–ionospheric–thermospheric domain. The initial, main and recovery stages of ionospheric storms are often discussed in terms of the variations of the two main ionospheric parameters *foF2* and *hmF2*, as obtained by ionograms recorded by ionosondes covering a large range of geomagnetic latitude (Cander and Mihajlovic, 1998; Blagoveshchensky et al., 2006). Moreover, severe ionospheric disturbances originating from solar flares have significant effects on the propagation of radio waves over the entire radio spectrum, on which radio communications and navigation systems critically depend (Thomson et al., 2004).

For these reasons in recent years real-time monitoring of the ionospheric plasma by ionosondes, together with the immediate availability of good-scaled data has become crucial. Since the 1980s several groups of researchers in the ionospheric community have been devoting much work and time to developing appropriate algorithms to automatically scale the ionograms and output the standard ionospheric characteristics (Reinisch and Huang, 1983; Fox and Blundell, 1989; Igi et al., 1993; Tsai and Berkey, 2000; Ding et al., 2007). The problems faced by these researchers are varied and complex and still today extensive effort is invested in continuously upgrading these programs in order to steadily improve the reliability of the automatically scaled data (Reinisch et al., 2005; McNamara, 2006).

One of the difficulties that an autoscaling program has to deal with is that sometimes, when carrying out ionospheric soundings on ionograms, F2 traces at double the altitudes are visible. These second-order F2 layer reflections are due to the "second bounces" of the signal

* Corresponding author. Tel.: +39 06 51860330; fax: +30 06 51860397.
E-mail address: scotto@ingv.it (C. Scotto).

1364-6826/$ - see front matter © 2008 Elsevier Ltd. All rights reserved.
doi:10.1016/j.jastp.2008.05.012

between the ionosphere and the Earth and do not represent additional higher layers. Pierce and Mimno (1940) first discussed these high multiple reflections from the F2 layer at night and concluded that they were the result of suitable curvatures in the F2 layer producing focusing effects. Subsequently, Bowman (1964) showed that these multiple reflections were mainly due to ionospheric irregularities instead of focusing effects and found evidence of an occurrence peak at sunrise and in the equinoctial months. In the same work Bowman also notes that this occurrence seems to be unaffected by the transition from quiet conditions to severe storm conditions.

When an ionogram shows multiple reflections from the F2 layer computer programs able to perform an autoscaling of the ionogram trace can be misled and the second-order F2 layer reflection can be identified as first order. When this happens the *foF2*-scaled value is usually not affected by a significant error, on the contrary the *M*(*3000*)*F2* and the *MUF*(*3000*)*F2* are wrongly scaled and

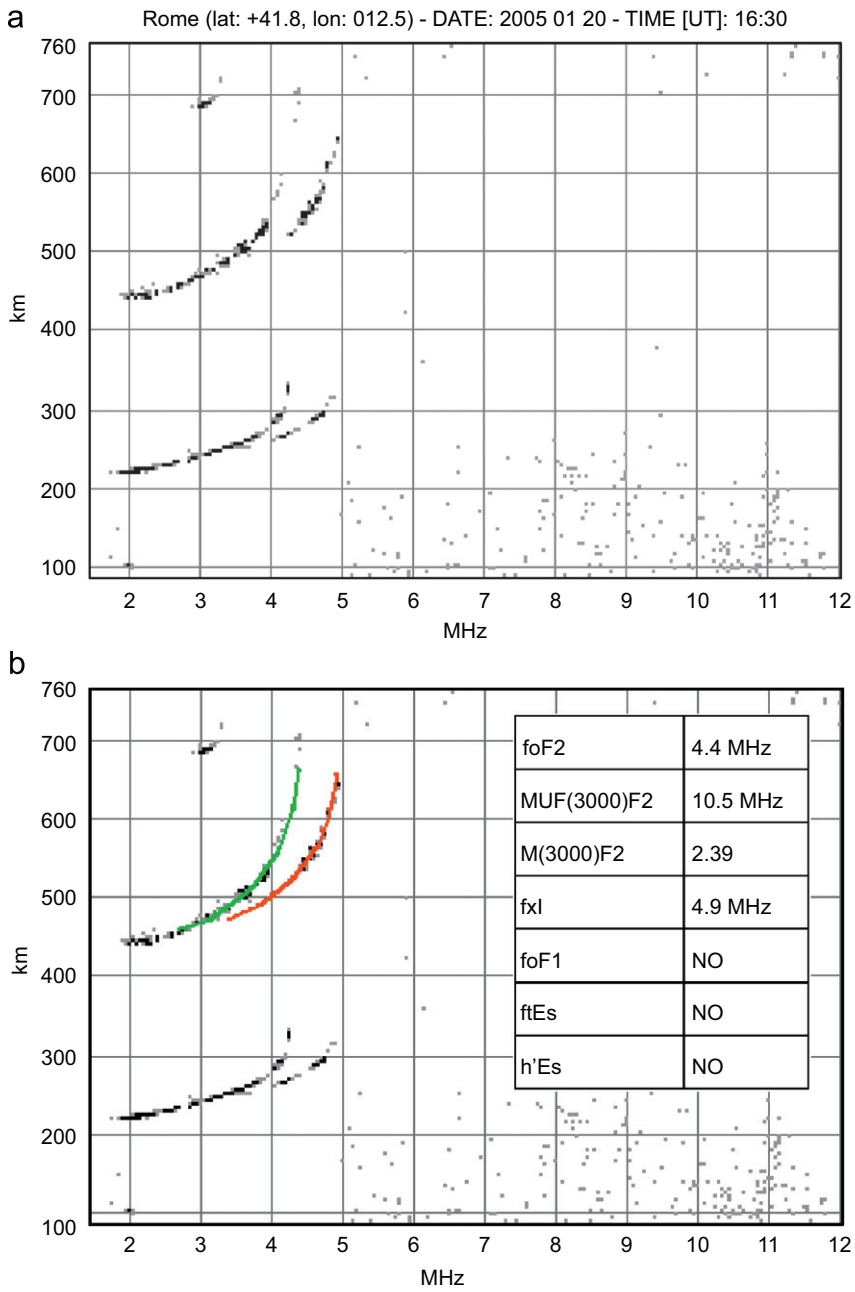

Fig. 1. (a) Ionogram recorded on 20 January 2005 at 16:30 UT by the AIS ionosonde installed at Rome for which (b) Autoscala was misled by the second-order F2 layer reflection, which is identified as first order. The automatically reconstructed traces are reported (the ordinary trace in green and the extraordinary trace in red).

as a consequence the electron density profile given as output is misrepresented.

Fox and Blundell (1989), Igi et al. (1993), and Tsai and Berkey (2000) discussed this issue in their works, nevertheless all of them underlined the fact that this process becomes important in determining whether or not the F trace is completely blanketed or overlapped by Es multiple traces without considering the cases in which only second-order F2 layer reflections are present. For instance Fox and Blundell included in their algorithm a check test for multiplicity of traces, looking for multiple Es layer traces overlapping with F layer traces.

The F2 layer identification performed by Autoscala (Pezzopane and Scotto, 2004) is not affected by characteristically flat Es multiple reflections, because the algorithm is designed to recognise the typical vertical asymptotical behaviour of the F2 traces (Pezzopane and Scotto, 2007). On the contrary Autoscala can be misled by multiple reflections from the F2 layer.

Fig. 1 is a typical example of an ionogram, recorded by the AIS ionosonde (Zuccheretti et al., 2003) installed at Rome, for which only multiple reflections from the F2 layer are visible; in this case Autoscala wrongly identified the second-order F2 layer reflection as first order.

This work describes a simple filter to smooth out this problem making the Autoscala output more reliable.

2. The identification of the second-order reflection

The basic idea of the filter is to compare the images contained in two sliding rectangles (see Fig. 3a) whose points are placed on the ionogram at virtual heights $h_{(u)}$ and $h_{(l)}$ ((u) and (l) standing for upper and lower, respectively), with the condition

$$h_{(u)} = 2h_{(l)} \tag{1}$$

and at frequency f. The side $d_{h(l)}$ in height of the lower rectangle is 103 km, the side $d_{h(u)}$ in height of the upper rectangle is 206 km, and the side d_f in frequency of both rectangles is 2.3 MHz. Hence as is also evident from Fig. 3a, $d_{h(u)}$ is twice $d_{h(l)}$, so that the filter takes into account the vertical stretch undergone by the second hop trace. The two rectangles are slid on the ionogram by varying the frequency of their centres from $(f_i+d_f/2)$ to $(f_f-d_f/2)$, the virtual height of the centre of the lower rectangle from 170 km to $[(h_f-d_{h(l)}/2)/2]$, and consequently the virtual height of the centre of the upper rectangle from 340 to $(h_f-d_{h(l)}/2)$, according to (1); h_f, f_i, and f_f, are the final height of the sounding, the initial frequency of the sounding, and the final frequency of the sounding, respectively. At each sliding step the images contained in the two rectangles are compared and if they are similar the image in the upper rectangle is considered as a second-order reflection trace, and at the end of the sliding process it is sensibly deleted from the ionogram.

In order to apply this idea, it is necessary to introduce a method to compare these two images and to establish whether they are similar or not. The correlation method is used, a technique widely applied for digital image processing (Vijaya Kumar et al., 2005; Stahlberg et al., 2002). As shown in Fig. 2, the grey-level value (the echo amplitude received by the AIS ionosonde is represented as a grey-level value, the darker the value, the stronger the echo amplitude received) of each image is acquired on two vectors x_i, and y_i, where $i = 1, \ldots, N$, and N represents the number of corresponding points contained in the rectangles. The correlation r is then calculated as follows:

$$r = \frac{N\sum_{i=1}^{N} x_i y_i - \sum_{i=1}^{N} x_i \sum_{i=1}^{N} y_i}{\sqrt{\left[N\sum_{i=1}^{N} x_i^2 - \left(\sum_{i=1}^{N} x_i\right)^2\right]\left[N\sum_{i=1}^{N} y_i^2 - \left(\sum_{i=1}^{N} y_i\right)^2\right]}}. \tag{2}$$

In order to assess whether the two images are similar or not, a threshold is fixed for r.

Fig. 3 illustrates how the application of this method to the ionogram of Fig. 1 allows Autoscala to correctly identify the first-order reflection instead of the second. Comparing the two figures it is worth noting that while the values of *foF2* differ only by 0.1 MHz, the values of *M(3000)F2* and *MUF(3000)F2* are significantly different.

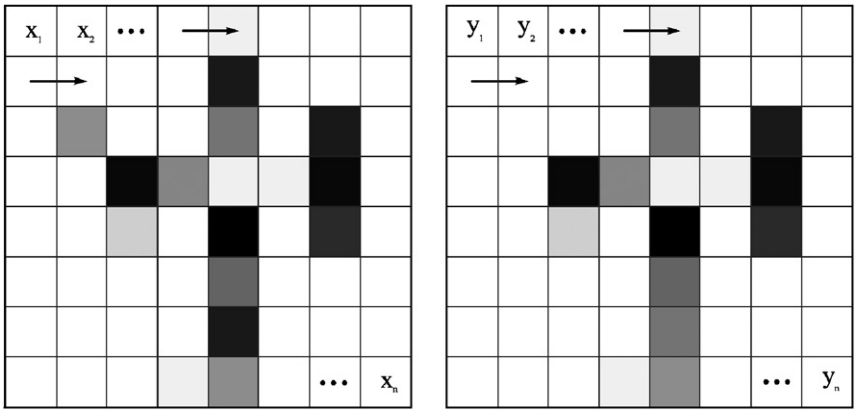

Fig. 2. The method used to compare two images. The grey-level value of each image is acquired on two vectors x_i, y_i, and the correlation r is computed according to Eq. (2). The two images are considered similar if r exceeds a fixed threshold.

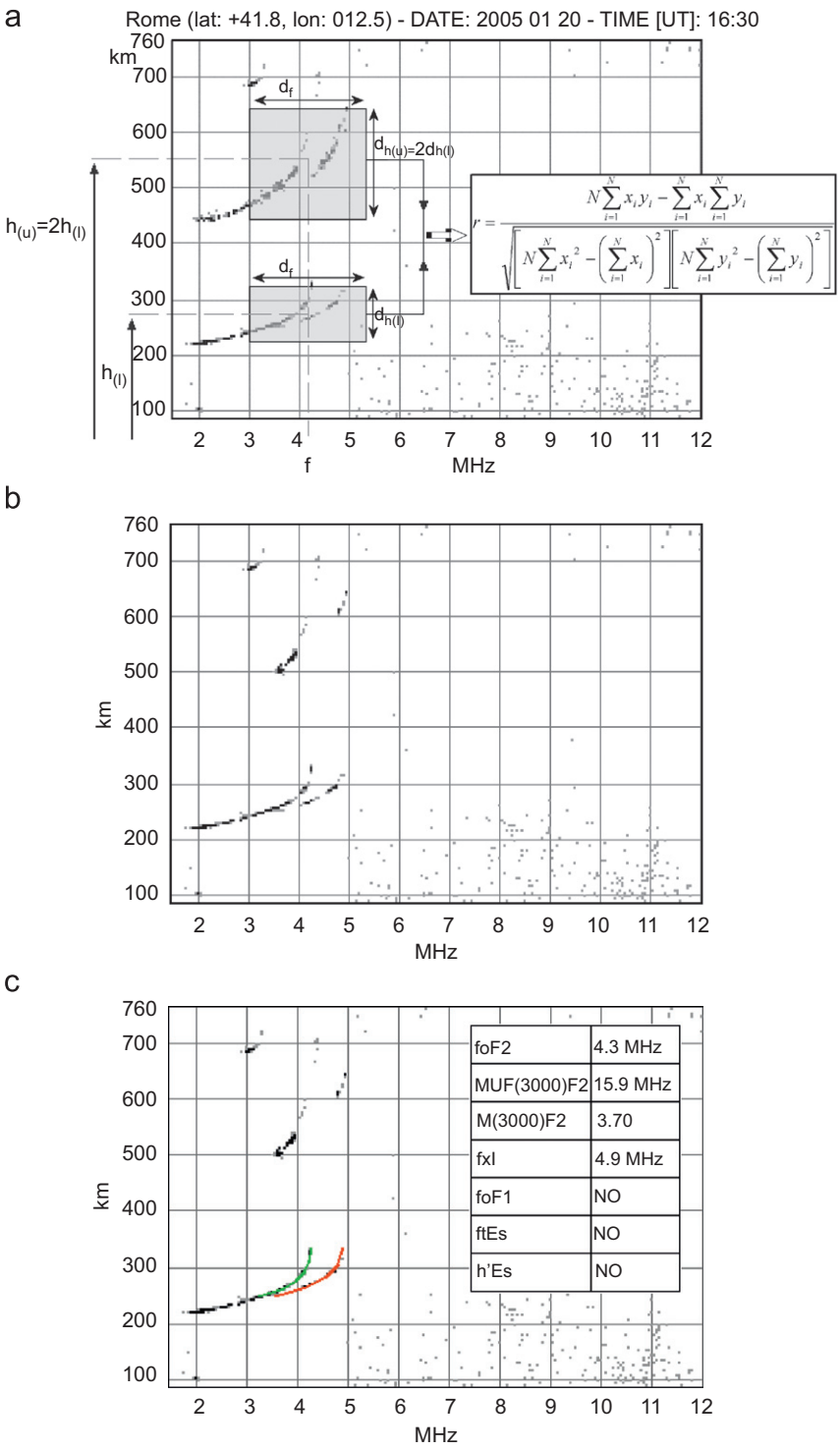

Fig. 3. (a) Application of the filter to the ionogram of Fig. 1. Two sliding rectangles are placed on the ionogram at virtual heights $h_{(u)}$ and $h_{(l)}$, with the condition $h_{(u)} = 2h_{(l)}$, and at frequency f. If the images contained in the two rectangles are similar the image in the upper rectangle is considered as a second order reflection trace. (b) The ionogram as it appears after deleting the identified second order reflection. (c) The correct autoscaling performed by Autoscala on the filtered ionogram. The automatically reconstructed traces are reported (the ordinary trace in green and the extraordinary trace in red).

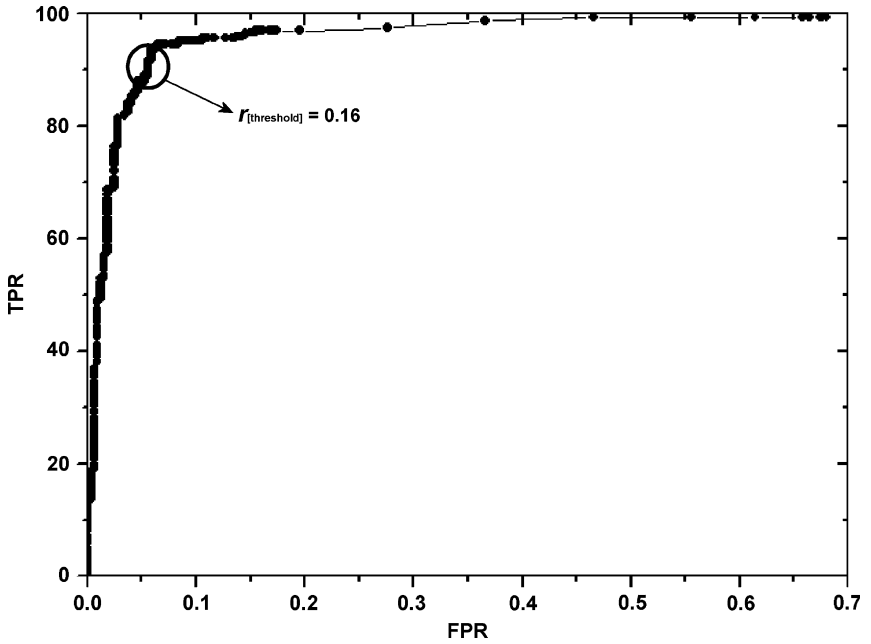

Fig. 4. ROC curve obtained from the data analysis. According to this curve the threshold of r was definitively set to 0.16.

3. ROC curve method: selection of the *r* threshold and performance of the filter

In signal detection theory, a receiver operating characteristic (ROC) curve is a graphical plot of the true positive rate (TPR) vs false positive rate (FPR) for a binary classifier system, as its discrimination threshold is varied.

Each point on the ROC curve represents a TPR/FPR pair corresponding to a particular decision threshold. A test with perfect discrimination has a ROC curve that passes through the upper left corner (100% TPR, 0% FPR) of the plot. As a consequence, the closer the ROC plot is to the upper left corner, the higher the overall accuracy of the test.

Regarding our problem, a dataset of 32,626 ionograms recorded in 2006 by the AIS ionosonde installed at Rome was considered. Within this dataset a population A of ionograms for which Autoscala was deceived because the second-order F2 layer reflection was identified as first order and a population NA of ionograms not affected by this problem were defined. For each possible value of the threshold, a fraction of ionograms belonging to A is correctly classified by the filter as positive (TP = true positive), while the rest of A is incorrectly classified by the filter as negative (FN = false negative). Similarly, for each possible value of the threshold, a fraction of ionograms belonging to NA is correctly classified by the filter as negative (TN = true negative), while the rest of NA is incorrectly classified as positive (FP = false positive).

The ROC curve can quantify, in terms of TPR = TP/(TP+FN) and FPR = FP/(FP+TN), the overall effectiveness of the correlation r to correctly discriminate the two populations A and NA of ionograms.

Table 1
Results TP and FN for the population A, and results TN and FP for the population NA, by applying the filter with the decisional threshold of r set to 0.16

Total number of ionograms: 32,626			
Population A		Population NA	
TP	FN	TN	FP
357	32	32219	18

An high percentage [TP/(TP+FN) = 92%] of second hop F2 traces that previously deceived Autoscala were successfully removed by the filter.

Fig. 4 shows the ROC curve for the binary classifier described in this work. According to this curve the threshold of r was definitively set to 0.16.

Table 1 presents the results TP and FN obtained for the population A, and the results TN and FP obtained for the population NA, after applying the filter with the decisional threshold set to 0.16. It emerges that the filter successfully deleted a high percentage [TP/(TP+FN) = 92%] of second hop F2 traces that previously deceived Autoscala.

4. Conclusions

This paper proposes a simple method to identify and delete an F2 second-order reflection trace in an ionogram. The tests performed showed that the application of this filter improves Autoscala's reliability.

A routine containing the filter was added to the new version of Autoscala running on the ionograms recorded by the AIS-INGV ionosondes installed at Rome

(41.8N, 12.5E; http://ionos.ingv.it/Roma/latest.html), Gibilmanna (37.9N, 14.0E; http://ionos.ingv.it/Gibilmanna/latest.html), and Tucuman stations (26.9S, 294.6E; http://www.ionos.ingv.it/Tucuman/latest.html).

References

Blagoveshchensky, D.V., MacDougall, J.W., Piatkova, A.V., 2006. Ionospheric effects preceding the October 2003 Halloween storm. Journal of Atmospheric and Solar Terrestrial Physics 68 (7), 821–831.

Bowman, G.G., 1964. Ionospheric irregularities and high multiple reflections. Australia Journal of Physics 17, 480–489.

Cander, L., Mihajlovic, S.J., 1998. Forecasting ionospheric structure during the great geomagnetic storms. Journal of Geophysical Research 103 (A1), 391–398.

Ding, Z., Ning, B., Wan, W., Liu, L., 2007. Automatic scaling of F2-layer parameters from ionograms based on the empirical orthogonal function (EOF) analysis of ionospheric electron density. Earth, Planets and Space 59 (1), 51–58.

Fox, M.W., Blundell, C., 1989. Automatic scaling of digital ionograms. Radio Science 24 (6), 747–761.

Igi, S., Nozaki, K., Nagayama, M., Ohtani, A., Kato, H., Igarashi, K., 1993. Automatic ionogram processing systems in Japan. In: Proceedings of Session G4 at the 24th General Assembly of the International Union of Radio Science (URSI), Kyoto, Japan, 25 August–2 September.

McNamara, L.F., 2006. Quality figures and errors bars for autoscaled Digisonde vertical incidence ionograms. Radio Science 41, RS4011.

Pezzopane, M., Scotto, C., 2004. Software for the automatic scaling of critical frequency foF2 and MUF(3000)F2 from ionograms applied for the ionospheric observatory of Gibilmanna. Annals of Geophysics 47 (6), 1783–1790.

Pezzopane, M., Scotto, C., 2007. Automatic scaling of critical frequency foF2 and MUF(3000)F2: a comparison between Autoscala and ARTIST 4.5 on Rome data. Radio Science 42 (4), RS4003.

Pierce, J.A., Mimno, H.R., 1940. The reception of radio echoes from distant ionospheric irregularities. Physical Review 57, 95–105.

Reinisch, B.W., Huang, X., 1983. Automatic calculation of electron density profiles from digital ionograms 3. Processing of bottomside ionograms. Radio Science 18 (3), 477–492.

Reinisch, B.W., Huang, X., Galkin, I.A., Paznukhov, V., Kozlov, A., 2005. Recent advances in real-time analysis of ionospheric drift measurements with digisondes. Journal of Atmospheric and Solar Terrestrial Physics 67 (12), 1054–1062.

Stahlberg, H., Zumbrunn, R., Engel, A., 2002. Digital Image Processing in Natural Science and Medicine. Available on line at 〈http://www.amp.ucdavis.edu/index.php?p=teachhenningDIP〉.

Thomson, N.R., Rodger, C.J., Dowden, R.L., 2004. Ionosphere gives size of greatest solar flare. Geophysical Research Letter 31, L06803.

Tsai, L.C., Berkey, F.T., 2000. Ionogram analysis using fuzzy segmentation and connectedness techniques. Radio science 35 (5), 1173–1186.

Vijaya Kumar, B.V.K., Mahalanobis, A., Juday, R.D., 2005. Correlation Pattern Recognition. Cambridge University Press, UK, 412pp.

Zuccheretti, E., Tutone, G., Sciacca, U., Bianchi, C., Arokiasamy, B.J., 2003. The new AIS-INGV digital ionosonde. Annals of Geophysics 46 (4), 647–659.